



# New Simple Modification of Dip, Spray and Cathodic Electrodeposition Coating Methods for Wire Coating (3D Coating)

Hisham R. Sadig<sup>1,2</sup>, Li Cheng<sup>1,\*</sup> and Xiang Tengfei<sup>1</sup>

<sup>1</sup>Nanjing University of Aeronautics and Astronautics, Material Science and Technology, Nanjing 210016, China

<sup>2</sup>Karary University, Chemical Engineering Department, Khartoum, Sudan

**Abstract:** In the current paper three most applied coating methods modified to suit wire coating (three dimensional coating). Capillary-gravitational coating (CGM) with natural motions considered to compensate the lifting of substrates, which normally occurs in the dip coating method. Besides a new economic-environmental friendly spray coating (EESM) assisted by the motor rotating to coat different wires, and branched cathodic electrodeposition (BCE) used also for the same mission. Thoroughly, several tests and evaluations carried out for those applied techniques. Remarkably, easy application detected for all modified methods. Unusually perfect morphology output and functional layers were synthesized. Comparison of all mentioned methods carried out considering loses and the number of coating time. Evaluation analysis has been comprehensively considered to find out capability of using these methods later on in the future.

Received on 20-10-2018  
Accepted on 16-11-2018  
Published on 14-03-2019

**Keywords:** Capillary-gravitational, environmental, modification, evaluation, spray, coating.

DOI: <https://doi.org/10.6000/2369-3355.2018.05.03.1>

## 1. INTRODUCTION

Concerning the rising demands in the coating-relied applications, and for further satisfaction of different functions, the art of coating emerged dramatically. Consequently, many experiments have been work on to get different purposes mainly, protection [1-4], isolation, inorganic anti-corrosion pigments[5], energy and solar cell application [6-10], moreover, sensor functions [11-14] different of coating methods have been technologically improved for deposition of thin layers on substrates via numerous techniques such as spin coating, wet chemical processes, roll-to-roll coating, dip coating, spray coating, and electrodeposition [15-17] each method has diverse gains and drawbacks. Such as, spin coating which is suitable for small, symmetrical, and flat substrates [18, 19]. The roll-to-roll coating is another method for large area coating, but need a flexible type of substrate [20]. Among these methods, dip coating [21, 22], spray coating [23, 24], and electrodeposition [25-27] are another options for deposition of thin films on a different kind of substrates.

### 1.1. Dip Coating

More attention has attracted by dip coating method than other methods, for its easiness of use and it's beneficial for both

academic research and industrial production; it also permits for the production of consistent coatings on various type of substrates [10, 28]. In addition to the ability of applied to all kinds of materials, along with an extensive variety of dispersed materials [29]. However, the notable disadvantage of this coating method is the consumption of a huge amount of solution which represented as the major shortcoming of the dip coating method, so its requests a large volume of solution to coat a big substrate. This consequently caused the waste of a bulk of the solution, which is objectionable for large-scale industrial requirements, especially when the solution is igneous or costly. Therefore, must be considered in comparison to other coating techniques [30, 31].

### 1.2. Spray Coating

The spray coating method has an unlimited potential for large scale fabrication, since the method has no restriction on the size of the substrate and low utilization of polymers, encouraging to substitute the conventional process which is spin coating methods [6]. The ability to access a wide-ranging spectrum of fluids with various morphologies, making the production of fully spray coated devices. But the thickness can be very inhomogeneous [31], which prohibits coating thicknesses, in addition, some parameters limited its qualification, like, the nozzle to substrate distance, flow rate, pressure, and substrate temperature, concentration of the mixture solution, spray duration, co-solvent mixture and number of times of sprayed [6].

\*29 Yudao St. Nanjing 210016, China; Tel: + 86 25 52112902, 13186405780; E-mail: licheng@nuaa.edu.cn

### 1.3. Cathodic Electrodeposition

Electrodeposition has arisen as an alternative with perfect features candidates for thin film synthesizing including the cathodic electrodeposition. Because it offers some impressive gains that consider it valuable method, etc. (i) the deposition achieved at low temperature and atmospheric pressure, (ii) it is a low-cost method which requires only simple apparatus. (iii) The film thickness can directly monitor by the charge consumed during the deposition process. The main disadvantage is the application limited just in using conducting substrates [32-35].

In this work, the modifications of the mentioned coating methods have motivated according to the reported drawbacks. In addition, the as-made improvements were suitable for wire coating. Repeatability of coating process tested thoroughly for the three methods, consequently, capillary-gravitational coating show perfect result. The new calculating approach illustrated that the economic-environmental friendly spray method has an ideal nozzle distance. Branched cathodic electrodeposition offered thin and nanostructured films. Moreover, the environmental impacts limitations considered in the techniques by adding simple ideas.

## 2. EXPERIMENTAL

### 2.1. Capillary-Gravitational Coating Method (CGM)

This coating process has a new idea emerged from the phenomena of capillary rise of the solution which depend upon surface tension [36], and the gravitational force. Systematically, the procedure depends upon immersing process, assisted by different motions in an upward direction (capillary rise) and downwards (gravitational drainage) without lifting substrate from the coating solution which happens in conventional dip coating method.

The equipment fabricated from tow plastic cone the bigger one represented the operative container while the smaller (narrow) used as capillary cone, in which Wires inserted, contacted to the solution and rotated by small motors (here; rotation benefit keeping the solution homogenous), the container attached vertically to barrier (to make the gravitational force as main effective force vs capillary) and to act as the main container from which the solution discharges using control valve., more illustration is shown in Figure 1.

### 2.2. Economic-Environmental Friendly Spray Coating (EESM)

The process of the coating was dependent on one side opened cone which hitched vertically with the motor, Figure 2 demonstrates the new approach. The opened section here allowed the sprayer to drive the solution into the cone, where the substrates positioned, save some of the solution collided the wall of cone, and provide safety in hindering the solution

drops and sprayed to mix with air around the targeted substrates, consequently save the environment from the may be-toxic or effective material. The motor used for rotating the wire electrodes for ensuring proper distribution of the coating solution on the surface of the wire.

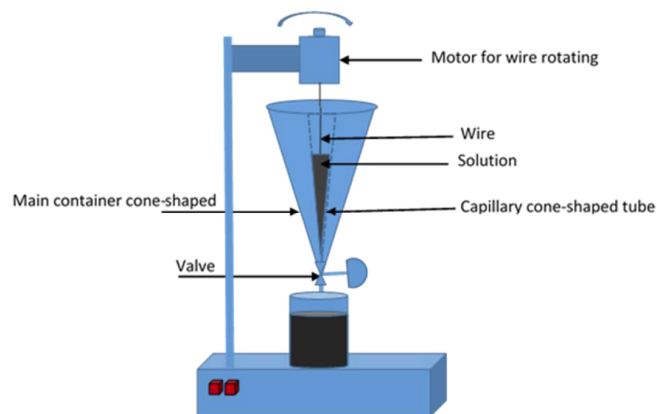


Figure 1: Show the equipment of capillary- gravitational coating method that used in this work.

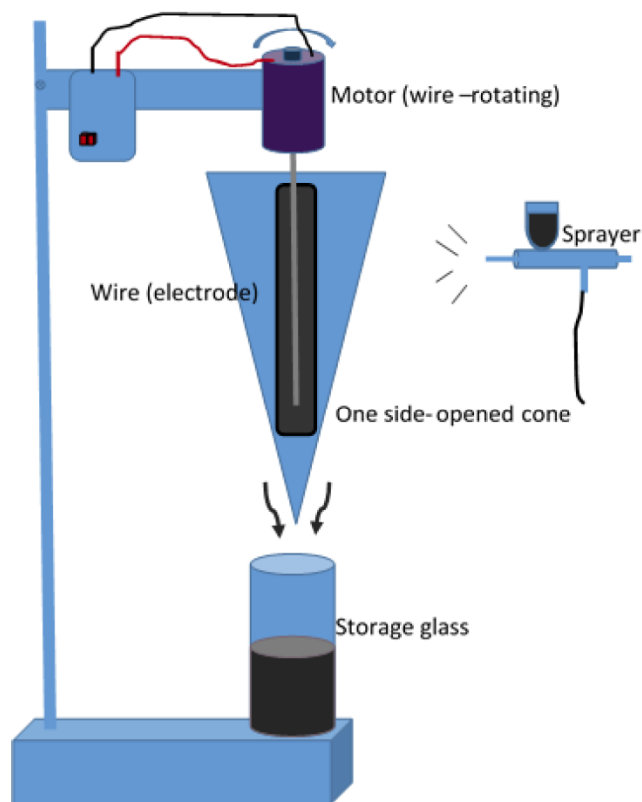
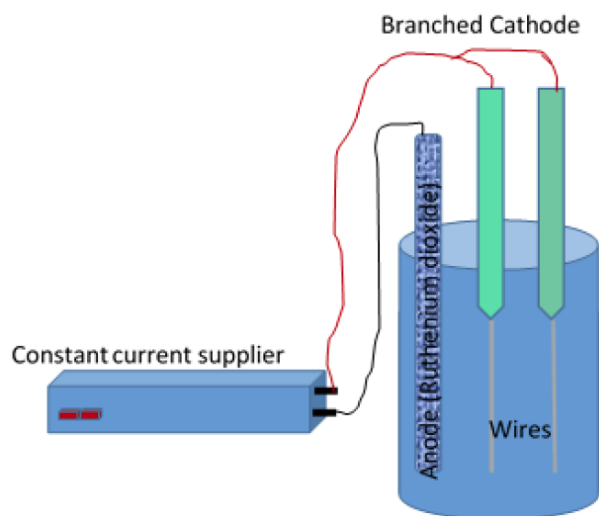


Figure 2: Illustrates the economic-environmental friendly spray coating method.

### 2.3. Branched Cathodic Electrodeposition (BCE)

For the branched cathodic electrodeposition, a lab-made electrodeposition bath capable of accommodating a solution volume of 20ml equipped. A ruthenium oxide mesh electrode utilized as the anode, a constant current of 4A/dm<sup>3</sup>

functioned to the electrodes. Electrodeposition was run out for 10 min at room temperature 21°C under the stirring condition of the solution, so as not to generate an emptiness on the electrode surface. At the end of the electrodeposition process, the electrodes were washed with deionized water. Sequentially dried with hot compressed air. Figure 3 Demonstrated the branched cathode. It was fabricated from the double plastic cone, the small one attached inside and bottom of the big one, wire electrodes inserted at the end of the hole of both cones. Foil sheets used as the conductive wires to supply the demanded current to the cell, then; the temperature, and all pH performance parameters test carried out.



**Figure 3:** Demonstrates the branched cathodic electrodeposition method.

### 3. RESULT AND DISCUSSION

#### 3.1. Films Structure Characterization

SEM investigation characteristics of fabricated layers by the three methods on both titanium and steel wires were implemented involving morphology, adhesion, and thickness of constructed films after cutting the wires into small samples. Images of SEM showed the morphology of oxide films in Figure 4. According to these images, the film oxides which fabricated by CGM were formed homogeneously along the length of the substrate. The coating's adhesion was respectable this appeared in the remaining of these oxides free of cracks and scratches, although; the heat treatment which exposed to them. All thickness has been measured using digital-micrograph software, CGM produces different thickness oxide films ranged between 0.79-2.97µm for Ti and steel substrates; respectively. The pattern of the oxide film gives rutile-type structure, amorphous. The thicknesses of the layers formed by EESM, the thickness were 1.9-3.68 and 1.5-7.1µm for titanium and steel electrodes correspondingly. The microstructure of the sensitive layer is fine-grained and homogenous with sandy-shape and significant porosity, as presented in Figure 4 the thickness of BCE were 2.5µm and

2.8µm for the same substrates (titanium and stainless steel) correspondingly.

#### 3.2. Functional Performance

The sensing function of the fabricated films was tested by subjecting the coated electrodes to the lab-made and commercial buffer solutions. Then the performance assessed according to matching the sensitivity behavior of as-prepared coated electrodes with Nernstian sensitivity on one side and comparing that with uncoated wire substrates on the other side. Figure 5 demonstrates all mentioned electrodes' sensitivity. From this figure it clear that the coated electrodes act with a close manner to the Nernstian behavior which characterized by the slope of 59.1mV/pH, while uncoated ones were far-off from that manner. The titanium coated by CGM coating method has provided slopes ranged between 58-59.86mV/pH, titanium coated by the EESM slopes range was 58-59.95mV/pH and the coated by BCE slopes were 57.9-58.92 mV/pH these values are identical to which have been reported in [37-40], however; not similar to sub/super-Nernstian obtained values in [41, 42]. On the other side, uncoated wires' slopes were remain sub-Nernstian, with 31.7mV/pH and 11.5mV/pH for titanium and stainless steel respectively.

#### 3.3. Evaluation of the Used Coating Methods

The evaluation of the methods carried out individually later on received data put together to make some comparison.

##### 3.3.1. CGM Method

The CGM fundamentally, depends on the action of capillary and reaction of gravity effects on the solution motions. Those natural phenomena played the main role in casting the coating solution along the substrate's body.

In the phenomenon of capillary motion, the capillary tube is an original device used to validate exactly what relatively happen. In such phenomena, the adhesion arises between the liquid and the inner conducted wall pulling the liquid column up till there will be sufficient liquid for gravitational forces to overcome these intermolecular forces. The interaction between the liquid and the tube is proportionally related to the radius, whereas the weight of the solution is proportional to the square of the tube's radius. So, a thin tube will pull a liquid column upper than a large tube will, it's well-known that the inner solution molecules cohere satisfactorily to the outer ones. The height of the solution with capillary phenomena follows the Jurin's law [43].

$$h = 2\gamma \frac{\cos\theta}{\rho gr} \quad (1)$$

Where  $\gamma$  is the liquid-air surface tension (force/unit length),  $\theta$  is the contact angle,  $\rho$  is the density of the liquid (mass/volume),  $g$  is the local acceleration due to gravity (length/square of time), and the radius of the tube is  $r$ . Thus

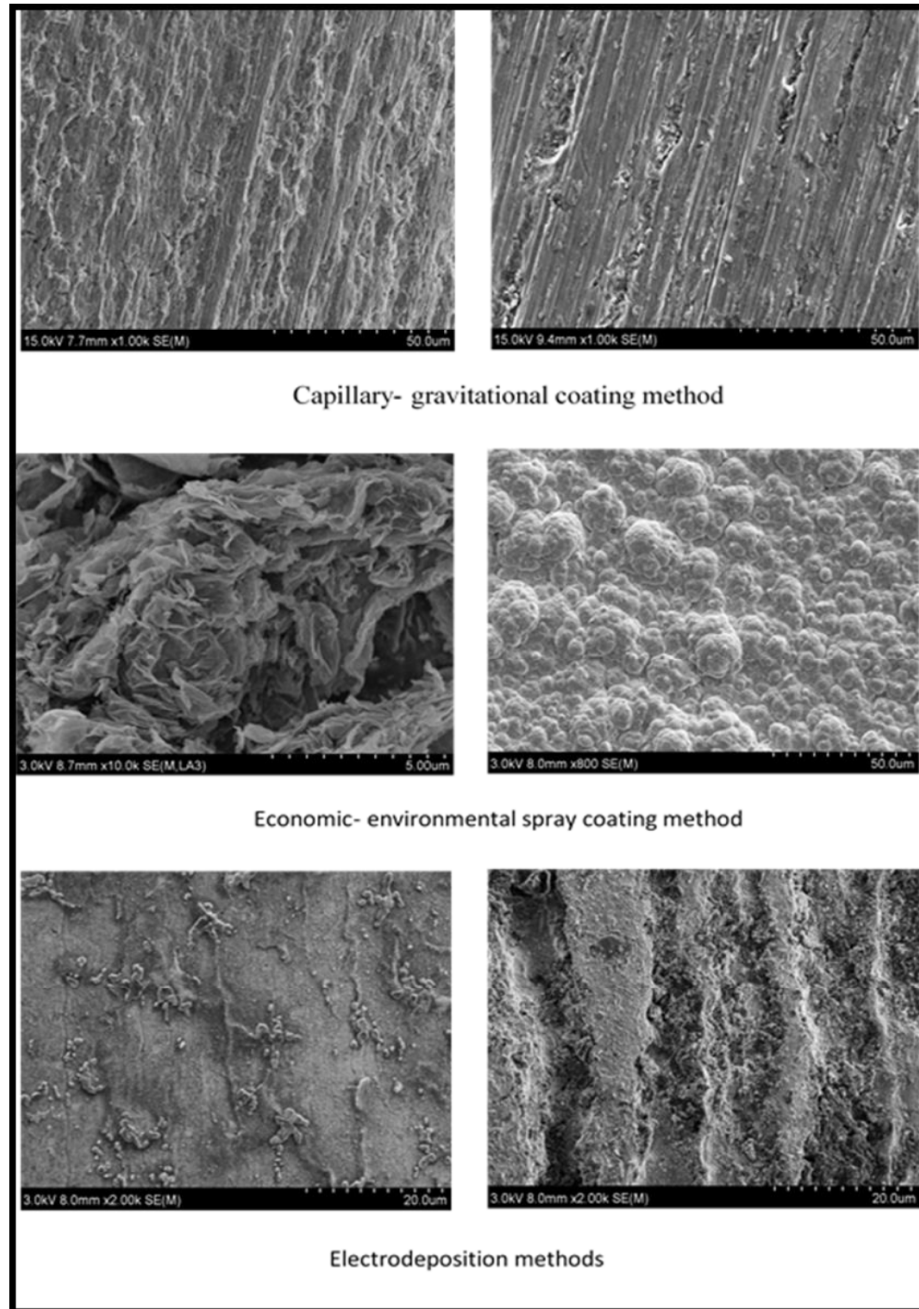


**Figure 4:** Explain the SEM images for structural characterization of all methods CGM, ESSM, and BCE.

the thinner the space in which the solution can travel, the further up it goes.

From the eq. (1) and using cone-shaped capillary tubes instead of tubes. And as it clear in Figure 6 the radius of tubes in our research isn't constant, it changes corresponding the gravity solution discharge direction supposing (no flow rate as the valve in closing case), also (there is no local acceleration due to gravity). Then by taking the equation (2). We can receive the relationship between h and r as it appears in equation (3).

$$V = \frac{1}{3}\pi r^2 h \quad (2)$$

For our cone-shaped capillary tube, the height that the coating solution will contact the substrates going up/downward will follow the equation (3).

$$h = \frac{3V}{\pi r^2} \quad (3)$$

Where the h represented the height of the solution inside the cone-shaped capillary tube, r is the diameter of the cone, and V is the volume of the cone. From equation (3) letting V at any time equal ( $\dot{v}$ ) the flow rate, then, the height can be calculated if the radius of the cone was given and vice versa, using the equation (4),

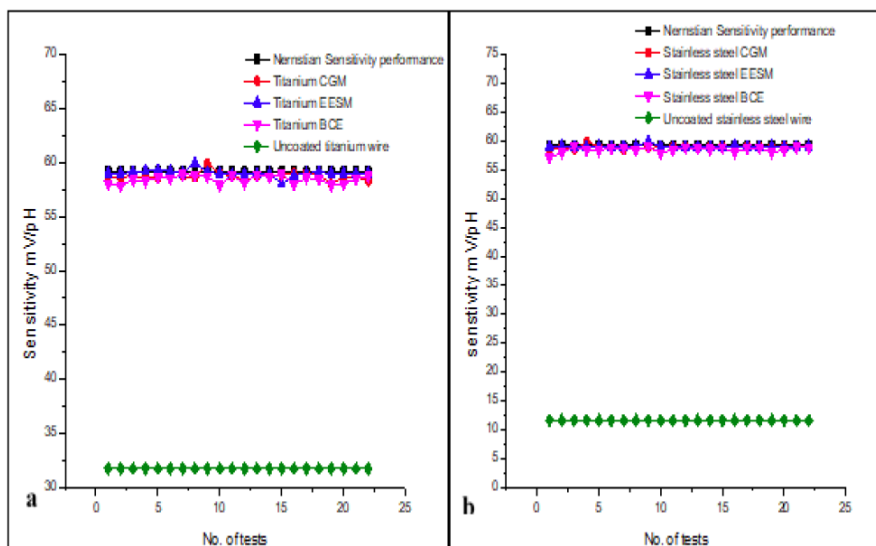


Figure 5: Shows the sensitivity of all fabricated electrode via the mentioned methods comparing with uncoated wires (a) titanium substrates (b) stainless steel substrates.

$$h = \frac{3V}{\pi r^2} \quad (4)$$

To study the impact of using the valve to control the flow rate of the coating solution, different six flow rate (20, 10, 6.67, 5, 4, and 3.33cc/min) were used experimentally to find which one will give good contact with our targeted wires (titanium and steel). Figure 6 shows the relation between the radius and the height in different flow rate, it clear that using the valve to reducing the flow rate provide much time for solution and electrodes to contact, and consequently coating do the step of up-going step. The next step is downward going which rely on solution motion according to the gravity. While this motion the valve played a vital role to delay this motion, giving more contacting opportunity. Consequently, the best flow rate was 33.33cc/min and the suitable time to complete the coating processing was 6min our practical time was 5min. here, it important to mentioned that, the capillary motion is responsible for making contact between the solution and the substrate, while the gravitational motion helps in discharging

of the solution supported by the valve. The targeted structure is determined due to the level of the coating solution extended in the contact with the substrate body.

Taking the volume of the coating solution under consideration the distance of the capillary tube to the bottom of the container emerged as influenced parameter that need to be controlled, Figure 7 gives more details how to move the capillary tube inside the container also more supplementary data in (Table 1).

### 3.3.2. The EESM Method

Evaluation of our new EESM coating method applied by using a new technique called; as the difference of circle-cone area test (DCCA) which used in our previous work [44], to fabricate pH sensor. The output of this method presented in Figure 8, the procedure have been governed by measuring the radius of distribution of dropped solution outside the cone after putting square papers behind it. We have considered the center of the cone as the center of all circles drawn as the base of calculations. Then the area of our one side-open vertical cone due to the direction of the process is considered

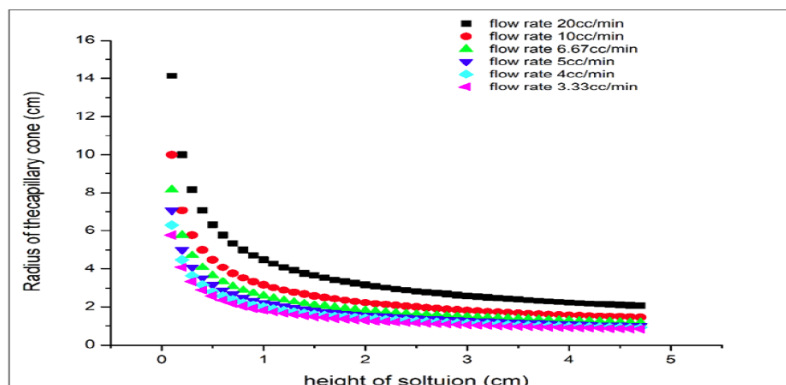
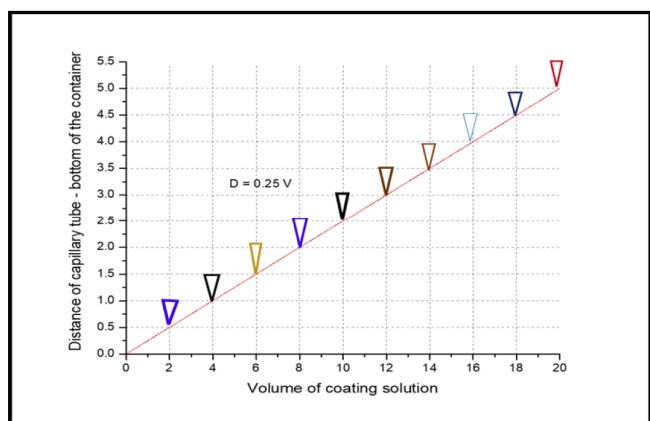


Figure 6: Shows evaluation of capillary- gravitational method using different flow rates.

**Table 1:** Shows the Volume of Coating Solution and the Distance of the Capillary Tube inside the Main Container

Volume of coating solution	Distance of capillary tube inside main container
20	5
18	4.5
16	4
14	3.5
12	3
10	2.5
8	2
6	1.5
4	1
0	0



**Figure 7:** Demonstrates the relationship between the distance of the capillary tube and bottom of the main container.

as a triangle and the area of all circles which was proportional to the distance of the sprayer nozzle from the substrates calculated. The difference of the two areas plotted with the distances (10, 15, 20, 25, and 30cm) and interpolated, also with a radius of the distributed solution on the square paper to provide the relation between them. This figure helps in the design of perfect coating and optimizing the ideal distance for reducing loses. The main idea here depends upon the fact that all solution outside of the cone considered as loses. So the calculation of the area difference denotes our ideal zero, in this point when the circle area equal the surface (triangle) area of the cone then the difference will equal to zero, and this will be the perfect distance. It represented here with the interaction of both curves distance with radius and distance with a difference of areas. According to our experiments and velocity (not included in the test just considered as constant), the ideal distance ranged between 12-15cm. The important observations were a negative and positive sign in results from subtracting areas; the negative denotes to the all solution poured inside the cone with access, while the positive sign means some of the solutions spilled outside the cone.

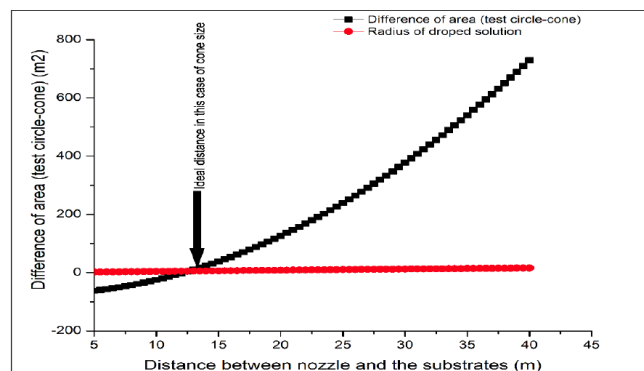


**Figure 8:** Shows the relation of nozzle to substrates distance and difference of area test circle and cone (capillary tube) and the ideal distance that was suitable for good condition of spray.

Losses of the solution was the remarkable issues in the EESM coating method which concerned by two factors, the first one is the distance of the nozzle from the substrates and the second one was air rushing. These mentioned factors affect in losing a considerable amount of the coating solution, however, using one side opened cone play a significant role to diminish the loses. Drops of solution that downfall on cone shaped tube wall help were collected at the end of the procedure. Here the recovering loses is important, the observation of loses due the distance > ideal distance was more than loses due the distance < ideal see the Figure 9, and (Table 2) this may for the first case effect of both parameters appears, while in the second case air rushing parameter effect can be negligible, for the small distance of nozzle.

**Table 2:** Illustrates the Distance of Nozzle to Substrates and Recovered Volume of Solution Accordingly

Distance of nozzle (cm)	Recovered volume (ml)
4	3
6	4
8	5
10	6
12	7
14	8
16	6
18	5
20	4
22	3
24	2
26	1
28	1
30	0.5

### 3.3.3. The BCE Method

The branched cathodic method is similar to the ordinary electrodeposition in all aspect the one difference was only

using branched cathode. The parameter that affects such method is the pH of the solution used as the electrolyte, the density of the current, the current efficiency, and the time needed for deposition.

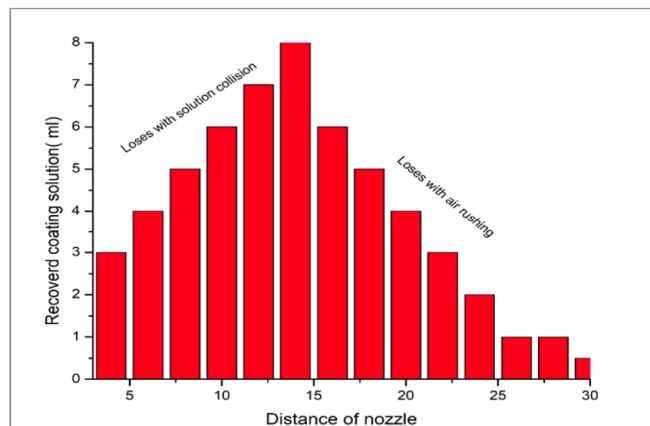


Figure 9: Explain the relation between nozzle to substrates distance and the recovered amount of coating solution.

The branched cathode was useful in coating two substrates at the same time. The evaluation of this method considered by the qualification of the solution vs. the number of coating times. It was observed that the solution after three time

become unreserved to coat more substrates. Finally, one can say that in all methods exceeding the solution amount could give a big number of coating times see the details in (Table 3). On the other side comparing all used methods Figure 10 explains that CGM has perfect linearity relation with the number of coating times with losing nearly constant volume of solution. Unlike the EESM and BCE, also EESM losing various volume of solution in each coating cycle, but more linear than BCE. The strange one was BCE which has no losing any volume of solution, but the impact of disqualification of the solution appears according to the change of the color and other characteristics due to repeating the process.

4. CONCLUSION

In addition to the advantages of dip, spray, and electrodeposition coating, our modifications were trustworthy to be considered. Those modifications will be expanded as effective coating method applying natural phenomena like capillary and gravitational, and other aspects like saving expensive materials and keeping the environment from pollutant that coming out while coating process. Furthermore, saving time in the coating process. In the current work the modified methods used to coat two different of wires (titanium and stainless steel) substrates. SEM images demonstrate the

Table 3: Shows the Overall Comparison of the all Methods

No. of the test	Titanium CGM	stainless steel CGM	Titanium EESM	stainless steel EESM	Titanium BCE	stainless steel BCE	Nernstian Sensitivity performance
1	65.3	64.2	56.2	56.4	58	57	59.16
2	63	62.4	56	56.2	57.8	58	59.16
3	62.4	61.7	56.8	57	58.4	59	59.16
4	61.5	60.8	56.9	56.7	58.3	58.4	59.16
5	60.9	60.5	58	57.8	58.6	58.3	59.16
6	60.3	60.1	58.65	58.3	58.5	58.8	59.16
7	60	59.8	58.9	58.7	58.9	58.75	59.16
8	59.7	59.6	59.8	60.1	58.83	58.4	59.16
9	58.69	58.89	61	60.8	58.7	58.89	59.16
10	57.8	57.6	62.2	62	57.9	57.87	59.16
11	56.4	56.5	63.6	62.5	58.82	58.4	59.16
12	56.5	53.2	58.5	58.92	58.1	58.88	59.16
13	56.64	53.6	56.64	56.25	58.85	58.73	59.16
14	57	54	59.18	59.2	58.63	58.56	59.16
15	58.01	54.6	58.82	56.8	58.92	58.87	59.16
16	59.5	56	53.4	52.5	57.97	57.98	59.16
17	59.7	57	60.28	61.36	58.57	58.69	59.16
18	60.4	59.8	58.29	58.94	58.45	58.8	59.16
19	60.8	60.3	58.83	57.3	57.95	57.94	59.16
20	61.3	61	54.2	52.5	58	58.4	59.16
21	64.4	62.6	59.02	58.5	58.48	58.96	59.16
22	65.1	63.2	61	60.1	58.76	58.8	59.16

adhesion of all fabricated films. Significant functionally outputs were observed according to the application of pH sensing. Evaluation of the coating methods carried out individually and comparison has been made to give a full sight of to how modification help in gaining more advantages. In the case of CGM, the best flow rate of the coating solution was 33.33cc/min and the good linearity relationship was obtained between the volume and the number of repeating coating process. In the case of EESM saving losing of the solution achieved using the Ideal distance approach the and found to be between 12-15cm. to overcoming the disqualification of the solution in the case of BCE there should be a method to regeneration the solution. Finally one can conclude the modification will help in the future to acquire more advantages.

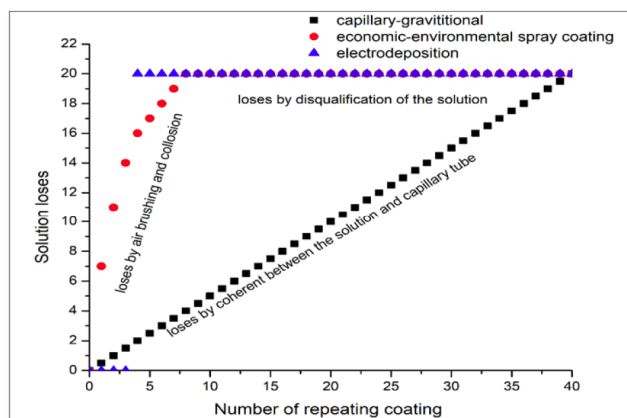


**Figure 10:** Shows the effect of number of repeating coating process on the solution loses in the all modified methods.

## ACKNOWLEDGEMENT

This work funded and supported by Priority Academic Program Development of Jiangsu Higher Education Institutions and Material science and technology college-Nanjing University of Aeronautics and Astronautics in China. Authors would like to provide sincere appreciation to funder and supporter also thanks, Karary University- Sudan.

## REFERENCES

- [1] Molin J, MP, Gimeno MJ, Izquierdo R, Gracenea JJ, Suay JJ. Influence of zinc molybdenum phosphate pigment on coatings performance studied by electrochemical methods. *Prog Org Coat* 2016; 97: 244-253. <https://doi.org/10.1016/j.porgcoat.2016.04.029>
- [2] Veg J, HS, Andersohn G, Oechsner M. Experimental studies of the effect of Ti interlayers on the corrosion resistance of TiN PVD coatings by using electrochemical methods. *Corros Sci* 2018; 133: 240-250. <https://doi.org/10.1016/j.corsci.2018.01.010>
- [3] Hernández LS, del Amo B, Romagnoli R. Accelerated and EIS tests for anticorrosive paints pigmented with ecological pigments. *Anti-Corrosion Methods and Materials* 1999; 46(3): 194-204. <https://doi.org/10.1108/00035599910273331>
- [4] Hofman R, JGFW, Pouwel I, Fransen T, Gellings PJ. FTIR and XPS Studies on Corrosion-resistant SiO<sub>2</sub> Coatings as a Function of the Humidity during Deposit ion. *Stud Surf Sci Catal* 1996; 24: 1-6.
- [5] Vesna B, MI Kovi, S. The mechanism of cathodic electrodeposition of epoxy coatings and the corrosion behaviour of the electrodeposited coatings. *J Serb Chem Soc* 2002; 67(5): 305-324. <https://doi.org/10.2298/JSC0205305M>

- [6] Aziz F, AFI. Spray coating methods for polymer solar cells fabrication: A review. *Mater Sci Semicond Process* 2015; 39: 416-425. <https://doi.org/10.1016/j.mssp.2015.05.019>
- [7] Hau SKY, Hin-Lap Z, Jingyu J, Alex KY. Indium tin oxide-free semi-transparent inverted polymer solar cells using conducting polymer as both bottom and top electrodes. *Org Electron* 2009; 10(7): 1401-1407. <https://doi.org/10.1016/j.orgel.2009.06.019>
- [8] Mashreghi A, MG. Investigating the effect of molar ratio between TiO<sub>2</sub> nanoparticles and titanium alkoxide in Pechini based TiO<sub>2</sub> paste on photovoltaic performance of dye-sensitized solar cells. *Renewable Energy* 2015; 75: 481-488. <https://doi.org/10.1016/j.renene.2014.10.033>
- [9] Reza Elyasi SMN, Namaghi HA, Ramezani N. Preparation and characterization of absorbing tubes with spectrally selective coatings using economical methods for low-to-mid-temperature solar thermal collectors. *Sol Energy Mater Sol Cells* 2015; 141: 57-70. <https://doi.org/10.1016/j.solmat.2015.05.021>
- [10] Inyoung Jang CK, Kim S, Yoon H. Fabrication of thin films on an anode support with surface modification for high-efficiency intermediate-temperature solid oxide fuel cells via a dip-coating method. *Electrochim Acta* 2016; 217: 150-155. <https://doi.org/10.1016/j.electacta.2016.09.065>
- [11] Mirzaei A, KJ, Hashemi B, Bonyani M, Leonardi SG, Neri G. Highly stable and selective ethanol sensor based on  $\alpha$ -Fe<sub>2</sub>O<sub>3</sub> nanoparticles prepared by Pechinisol-gel method. *Ceramics International* 2016; 42: 6136-6144. <https://doi.org/10.1016/j.ceramint.2015.12.176>
- [12] Wei L, JD, Qiuyun F, Dongxiang Z, Yunxiang H, Shuping G, Zhiping ZS. Nanocrystalline SnO<sub>2</sub> film prepared by the aqueous sol-gel method and its application as sensing films of the resistance and SAW H<sub>2</sub>S sensor. *Sens Actuators B* 2015; 217: 119-128. <https://doi.org/10.1016/j.snb.2014.10.078>
- [13] Libu M, KC, Jan K, Krzysztof Z, Dorota Szwagierczak GS. Sensing mechanism of RuO<sub>2</sub>-SnO<sub>2</sub> thick film pH sensors studied by potentiometric method and electrochemical impedance spectroscopy. *J Electroanal Chem* 2015; 759: 82-90. <https://doi.org/10.1016/j.jelechem.2015.10.036>
- [14] Pedro S, FJG-G, Francisco Y, Jorge G-R, González-Elipse AR. Characterization and application of a new pH sensor based on magnetron sputtered porous WO<sub>3</sub> thin films deposited at oblique angles. *Electrochim Acta* 2016; 193: 24-31. <https://doi.org/10.1016/j.electacta.2016.02.040>
- [15] Th. Pauporte, AG, Kahn-Harari A, de Tacconic N, Chenthamarakshanc R, Rajeshwar DLK. Cathodic electrodeposition of mixed oxide thin films. *J Phys Chem Solids* 2003; 64: 1737-1742. [https://doi.org/10.1016/S0022-3697\(03\)00122-7](https://doi.org/10.1016/S0022-3697(03)00122-7)
- [16] Casell IG, MC, Rosanna T. Anodic electrodeposition of iridium oxide particles on glassy carbon surfaces and their electrochemical/SEM/XPS characterization. *J Electroanal Chem* 2015 736: 147-152. <https://doi.org/10.1016/j.jelechem.2014.11.012>
- [17] Kyung-Hwa K, KSK, Gil-Pyo K, Sung-Hyeon B. Electrodeposition of mesoporous ruthenium oxide using an aqueous mixture of CTAB and SDS as a templating agent. *Current Applied Physics* 2012; 12: 36-39. <https://doi.org/10.1016/j.cap.2011.04.029>
- [18] Balzarotti R, Cristiani C, Francis LF. Spin coating deposition on complex geometry substrates: Influence of operative parameters. *Surface and Coatings Technology* 2017; 330: 1-9. <https://doi.org/10.1016/j.surfcoat.2017.09.077>
- [19] Baranowsk-Korczyk A, ARB, Kamil S, Tomasz Wojciechowski KF. The synthesis, characterization and ZnS surface passivation of polycrystalline ZnO films obtained by the spin-coating method. *J Alloys Compd* 2016; 295: 1-9.
- [20] Zhang R, et al. Soap-film coating: high-speed deposition of multilayer nanofilms. *Sci Rep* 2013; 3: 1477. <https://doi.org/10.1038/srep01477>
- [21] Dip-coating. Available from: "https://en.wikipedia.org/w/index.php?title=Dip-coating&oldid=81448491#8".
- [22] Toktam R, MHE. Achieving to a superhydrophobic glass with high transparency by a simple sol-gel-dip-coating method. *Surf Coat Technol* 2015; 276: 557-564. <https://doi.org/10.1016/j.surfcoat.2015.06.015>
- [23] Jungchan K, DS, Choonsoo K, Youngbin B, Byeongho L, Hee JK, Jong-Chan Lee JY. A high-performance and fouling resistant thin-film composite membrane prepared via coating TiO<sub>2</sub> nanoparticles by sol-gel-derived spray method for PRO applications. *Desalination* 2016; 397: 157-164. <https://doi.org/10.1016/j.desal.2016.07.002>

- [24] Soltani-Kordshuli F, FZ, Eslamian M. Graphene-doped PEDOT:PSS nanocomposite thin films fabricated by conventional and substrate vibration-assisted spray coating (SVASC). *Engineering Science and Technology an International Journal* 2016; 19: 1216-1223. <https://doi.org/10.1016/j.jestch.2016.02.003>
- [25] Jayakumar M, KAV, Sudha R, Srinivasan TG, Vasudeva Rao PR. Electrodeposition of ruthenium, rhodium and palladium from nitric acid and ionic liquid media: Recovery and surface morphology of the deposits. *Mater. Chem. Phys. Materials Chemistry and Physics* 2011; 128: 141-150. <https://doi.org/10.1016/j.matchemphys.2011.02.049>
- [26] Nur Kıcıra, Tunc, Tükena, Ozge Erkenb, Cebraıl Gumusc, Yuksel Ufuktepeca. Chemistry, Nanostructured ZnO films in forms of rod, plate and flower: Electrodeposition mechanisms and characterization. *Appl Surf Sci* 2016; 377: 191-199. <https://doi.org/10.1016/j.apsusc.2016.03.111>
- [27] Kwang MK, JHK, Yun YL, Kyoo YK. Electrodeposition of ruthenium oxide on ferritic stainless steel bipolar plate for polymer electrolyte membrane fuel cells. *International Journal of Hydrogen Energy* 2012; 37: 1653-1660. <https://doi.org/10.1016/j.ijhydene.2011.10.028>
- [28] Jianggao LS, Pengyang L, Mengjie F, Xinwang Y. A modified dip-coating method to prepare BN coating on SiC fiber by introducing the sol-gel process. *Surf Coat Technol* 2016; 286: 57-63. <https://doi.org/10.1016/j.surfcoat.2015.12.023>
- [29] Yu Z, GC, Yanyun Z. Investigation of different coating application methods on the performance of edible coatings on Mozzarella cheese. *LWT - Food Sci Technol Int* 2014; 56: 1-9. <https://doi.org/10.1016/j.lwt.2013.11.006>
- [30] Glynn C, *et al.* Linking Precursor Alterations to Nanoscale Structure and Optical Transparency in Polymer Assisted Fast-Rate Dip-Coating of Vanadium Oxide Thin Films *Sci Rep* 2015; 5: 11574.
- [31] Mousavi SH, *et al.* A novel wet coating method using small amounts of solution on large flat substrates. *Appl Surf Sci* 2017; 419: 753-757. <https://doi.org/10.1016/j.apsusc.2017.05.109>
- [32] Patake VD, CDL, Oh Shim J. Electrodeposited ruthenium oxide thin films for supercapacitor: Effect of surface treatments. *Appl Surf Sci* 2009; 255: 4192-4196. <https://doi.org/10.1016/j.apsusc.2008.11.005>
- [33] Metikoš-Huković M, Babić R, Jović F, Gruba Z. Anodically formed oxide films and oxygen reduction on electrodeposited ruthenium in acid solution. *Electrochim Acta* 2006; 51: 1157-1164. <https://doi.org/10.1016/j.electacta.2005.05.029>
- [34] Winiarski J, AL, Pohl P, Szczygiel B. The effect of pH of plating bath on electrodeposition and properties of protective ternary Zn-Fe-Mo alloy coatings. *Surf Coat Technol* 2016; 299: 81-89. <https://doi.org/10.1016/j.surfcoat.2016.04.073>
- [35] Shmychkova O, Tly, Amadelli R, Velichenko A. Electrodeposition of Ni<sup>2+</sup>-doped PbO<sub>2</sub> and physicochemical properties of the coating. *J Electroanal Chem* 2016; 774: 88-94. <https://doi.org/10.1016/j.jelechem.2016.05.017>
- [36] Bush PJWM, Capillary R. 18.357 Interfacial Phenomena, 2013.
- [37] Emad El-Deen M, El-Giar DOW. Microparticle-based iridium oxide ultramicroelectrodes for pH sensing and imaging. *J Electroanal Chem* 2007; 609: 147-154. <https://doi.org/10.1016/j.jelechem.2007.06.022>
- [38] Kuo L-M, *et al.* A precise pH microsensor using RF-sputtering IrO<sub>2</sub> and Ta<sub>2</sub>O<sub>5</sub> films on Pt-electrode. *Sens Actuators B* 2014; 193: 687-691. <https://doi.org/10.1016/j.snb.2013.11.109>
- [39] Jongman P, MK, Shinseon KM. Surface renewable nano-iridium oxide polymeric composite pHelectrodes. *Sens Actuators B* 2014; 204: 197-202. <https://doi.org/10.1016/j.snb.2014.07.104>
- [40] Xiao-Rong H, Q-qR, Xiao-Jun Y, Wei W, Wei C, Dong-Ping Z. Iridium oxide based coaxial pH ultramicroelectrode. *Electrochemistry Communications* 2014; 40: 35-37. <https://doi.org/10.1016/j.elecom.2013.12.012>
- [41] Libu M, KC, Jan K, Krzysztof Z, Dorota S, Robert PS. Fabrication of thick film sensitive RuO<sub>2</sub>-TiO<sub>2</sub> and Ag/AgCl/KCl reference electrodes and their application for pH measurements. *Sens Actuators B* 2014; 204: 57-67. <https://doi.org/10.1016/j.snb.2014.07.067>
- [42] Sardarinejad A, Maurya DK, Alameh K. The effects of sensing electrode thickness on ruthenium oxide thin-film pH sensor. *Sens Actuators A* 2014; 214: 15-19. <https://doi.org/10.1016/j.sna.2014.04.007>
- [43] Capillarity and Wetting Phenomena. Springer Science, 2004.
- [44] Sadig HR, Cheng L, Xiang T. Using sol-gel supported by novel economic and environment-friendly spray-coating in the fabrication of nanostructure tri-system metal oxide-based pH sensor applications. *J Electroanal Chem* 2018; 827: 93-102. <https://doi.org/10.1016/j.jelechem.2018.09.017>